

基于传递函数的超稳激光器光学参考腔热仿真研究

邓久昌^{1,2}, 谢永¹, 孟令强^{2,3*}, 边伟², 印雄飞², 贾建军^{1,2,3*}

¹中国科学院上海技术物理研究所空间主动光电重点实验室, 上海 200083;

²国科大杭州高等研究院物理与光电工程学院, 浙江省引力波精密测量重点实验室, 引力波宇宙太极实验室, 浙江 杭州 310024;

³之江实验室传感系统研究中心, 浙江 杭州 311121

摘要 当采用 Pound-Drever-Hall (PDH) 稳频技术将激光频率锁定在 Fabry-Pérot (FP) 腔时, 激光的频率稳定性完全取决于 FP 腔的腔长稳定性, 而外界环境的温度波动是参考腔腔长稳定性的重要影响因素之一。以典型的 FP 参考腔真空系统为研究对象, 着眼于参考腔对外界温度变化的响应情况, 通过理论分析推导出 FP 参考腔温度与外界温度的传递函数关系, 并基于参考腔的温度敏感度曲线, 给出参考腔温度敏感度的近似计算公式。数值计算结果证明了传递函数关系的正确性, 敏感度近似计算公式的结果虽与理论值存在一定误差, 但具有形式简单、参数直观、计算方便等特点, 对超稳激光系统设计具有重要的指导意义。

关键词 激光光学; FP 参考腔; 传递函数; 热屏蔽层; 温度敏感度

中图分类号 O433 文献标志码 A

DOI: 10.3788/AOS230460

1 引言

超稳激光具有极低的频率噪声、极高的相干性等特点^[1], 是高分辨率激光光谱学^[2]、光学频率精密控制^[3-4]以及精密测量物理^[5-6]的核心光源, 在冷原子光钟^[7-8]、测地学^[9]、引力波探测^[10-12]和光学频率传递^[13-14]等方面有着广泛的应用。超稳激光器通常基于 Pound-Drever-Hall (PDH) 激光稳频技术^[15-16], 使用高速电子学系统将可调谐激光光源的输出频率精准锁定在 Fabry-Pérot (FP) 参考腔的共振频率上。因此, FP 参考腔的腔长稳定性直接决定了输出激光的频率稳定性^[17-19]。FP 参考腔的温度波动作为腔长的主要影响因素之一, 如何快速对其温度特性进行分析一直是超稳激光器的研究热点。

FP 参考腔的腔长变化主要受外界环境的温度波动影响^[20-21], 为了抑制该影响, 国内外研究者通常将参考腔置于具有多个热屏蔽层的真空腔室内, 以获得较大的热时间常数和较低的温度敏感度^[22-23]。为了快速准确地分析真空腔室中的热屏蔽层参数对参考腔温度的影响, 国内外研究者利用不同的热分析方法进行了相应研究: Zhang 等^[21]利用有限元方法进行分析, 虽然该方法的计算精度较高, 但其有限元模型复杂且计算

速度较慢; 伍巍^[24]利用传递函数法进行分析, 得到 FP 参考腔的温度变化规律, 但没有作进一步的深入研究。以上研究者仅对参考腔系统的温度随时间变化的规律进行分析, 并没有在频域上对参考腔系统的温度敏感度进行研究。Dai 等^[20]运用直接微分法分析参考腔温度随外界温度的变化关系, 不仅对参考腔系统的温度随时间的变化规律进行了分析, 还对参考腔系统的温度敏感度曲线进行了进一步研究。但是该方法分别单独考虑了热传导或热辐射工况, 所得结果形式复杂, 温度敏感度与影响参数的关系不够直观, 而实际中必须考虑热传导、热辐射的综合作用。由此可见, 目前对于参考腔系统的热分析方法大部分仅针对参考腔温度随时间变化的规律进行了研究, 并且对于实际工况需要的参考腔温度敏感度进行分析的研究结果不能满足实际需求。因此, 本文提出一种综合考虑热传导及热辐射工况的参考腔热分析研究方法, 并建立了温度敏感度与系统物理参数的关系。

本文基于传递函数法对采用多个热屏蔽层设计的真空腔系统进行研究, 分析 FP 参考腔的热特性, 给出 FP 参考腔温度与外界环境温度的传递函数关系, 推导出参考腔温度敏感度的近似计算公式。所得结果可为实际工程中参考腔系统的设计提供参考。

收稿日期: 2023-01-10; 修回日期: 2023-02-20; 录用日期: 2023-03-06; 网络首发日期: 2023-03-13

基金项目: 国家自然科学基金(12103014)、国家重点研发计划(2021YFC2201800)

通信作者: *jjun10@mail.sitp.ac.cn; **lingqiang.meng@ucas.ac.cn

2 参考腔热特性理论分析

热传递主要有 3 种方式,即热对流、热传导和热辐射。由于 FP 参考腔通常被置于真空环境中,热对流作用微乎其微,因此,主要考虑热传导和热辐射^[25-26]。

以图 1 所示的具有多个热屏蔽层的 FP 参考腔系统为研究对象,系统中 P₀ 为真空室, P₁、P₂、P₃ 为热屏蔽

层, P₄ 为 FP 参考腔,真空室与屏蔽层及屏蔽层与参考腔之间由特氟龙 (teflon) 支撑柱连接。系统初始温度为 T₀,真空室 (P₀) 外部温度由初始温度 T₀ 变为 T_f 时,温度变化量 ΔT = T_f - T₀。根据文献[27]的传热学公式(热传导及热辐射),热屏蔽层 P₁、P₂、P₃ 以及 FP 参考腔 P₄ 的温度变化应满足

$$\begin{cases} C_1 \frac{dT_1}{dt} = \beta_{01}(T_f^4 - T_1^4) - \beta_{12}(T_1^4 - T_2^4) + \alpha_{01}(T_f - T_1) - \alpha_{12}(T_1 - T_2) \\ C_2 \frac{dT_2}{dt} = \beta_{12}(T_1^4 - T_2^4) - \beta_{23}(T_2^4 - T_3^4) + \alpha_{12}(T_1 - T_2) - \alpha_{23}(T_2 - T_3) \\ C_3 \frac{dT_3}{dt} = \beta_{23}(T_2^4 - T_3^4) - \beta_{34}(T_3^4 - T_4^4) + \alpha_{23}(T_2 - T_3) - \alpha_{34}(T_3 - T_4) \\ C_4 \frac{dT_4}{dt} = \beta_{34}(T_3^4 - T_4^4) + \alpha_{34}(T_3 - T_4) \end{cases}, \quad (1)$$

式中: $\alpha = \frac{kA}{L}$, 其中 k 表示导热系数, A 表示传热截面积, L 表示导热长度; $\beta = \frac{\sigma}{\frac{1}{A_1} \left(\frac{1}{\epsilon_1} - 1 \right) + \frac{1}{A_2} \frac{1}{\epsilon_2}}$, 其中

σ 表示斯蒂芬-玻尔兹曼常数, A₁、A₂ 分别表示辐射内表面和外表面的面积, ε₁、ε₂ 分别表示辐射内表面和外表面的辐射发射率; c_i、m_i、C_i = c_im_i、T_i 分别表示 P_i (i=1,2,3,4) 的比热容、质量、热容量和温度^[27]。

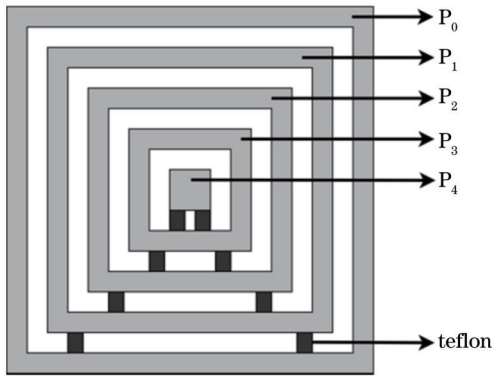


图 1 具有多个热屏蔽层的 FP 参考腔系统物理模型

Fig. 1 Physical model of FP reference cavity system with multilayer thermal shield

通过四阶-五阶 Runge-Kutta 算法求解上述一阶微分方程组^[28], 可得到温度变化情况。然而, 由于热辐射与温度的四次方有关, 很难直接建立 T_f 与 T_i 的传递函

数关系, 进而研究 FP 参考腔温度 T₄ 与 T_f 之间的温度敏感度关系。由分析结果可知, 当系统达到理想稳态时, 有 T_f = T_i, 且整个过程中满足 T_f - T_i ≤ ΔT, 据此可对热辐射项进行简化。例如, 对 T_f⁴ - T₁⁴ 进行展开, 可得

$$(T_f^4 - T_1^4) = (T_f^2 - T_1^2)(T_f^2 + T_1^2) = (T_f - T_1)(T_f + T_1)(T_f^2 + T_1^2) = a(T_f - T_1), \quad (2)$$

式中: $a = (T_f + T_1)(T_f^2 + T_1^2) = T_f^3 + T_1 T_f^2 + T_1^2 T_f + T_1^3$ 。当 ΔT 远小于 T_f 与 T₁ 时, 可近似认为 T_f ≈ T₁, 进而得到 a ≈ 4T_f³, 即 (T_f⁴ - T₁⁴) ≈ 4T_f³(T_f - T₁)。其他热辐射项同理简化。

据此, 对式(1)进行简化, 并对其进行拉普拉斯变换, 得到

$$\begin{cases} sC_1 \tilde{T}_1 = q_{01}(\tilde{T}_f - \tilde{T}_1) - q_{12}(\tilde{T}_1 - \tilde{T}_2) \\ sC_2 \tilde{T}_2 = q_{12}(\tilde{T}_1 - \tilde{T}_2) - q_{23}(\tilde{T}_2 - \tilde{T}_3) \\ sC_3 \tilde{T}_3 = q_{23}(\tilde{T}_2 - \tilde{T}_3) - q_{34}(\tilde{T}_3 - \tilde{T}_4) \\ sC_4 \tilde{T}_4 = q_{34}(\tilde{T}_3 - \tilde{T}_4) \end{cases}, \quad (3)$$

式中: β₀₁ = 4T_f³β₀₁ (其余各项同理); q 为热流量, q = β' + α; \tilde{T}_i 为 P_i (i=1,2,3,4) 的温度变化。

通过对式(3)进行求解, 得到 FP 参考腔温度变化 \tilde{T}_4 与 \tilde{T}_f 之间的传递函数, 即

$$\frac{\tilde{T}_4}{\tilde{T}_f} = \frac{q_{01}q_{12}q_{23}q_{34}}{a_4s^4 + a_3s^3 + a_2s^2 + a_1s + a_0}, \quad (4)$$

式中: $a_4 = C_1C_2C_3C_4$; $a_3 = C_2C_3C_4q_{01} + C_1C_3C_4q_{12} + C_2C_3C_4q_{12} + C_1C_2C_4q_{23} + C_1C_3C_4q_{23} + C_1C_2C_3q_{34} + C_1C_2C_4q_{34}$; $a_2 = C_3C_4q_{01}q_{12} + C_2C_4q_{01}q_{23} + C_3C_4q_{01}q_{23} + C_1C_4q_{12}q_{23} + C_2C_3q_{01}q_{34} + C_2C_4q_{01}q_{34} + C_2C_4q_{12}q_{23} + C_3C_4q_{12}q_{23} + C_1C_3q_{12}q_{34} + C_1C_4q_{12}q_{34} + C_2C_3q_{12}q_{34} + C_2C_4q_{12}q_{34} + C_1C_2q_{23}q_{34} + C_1C_3q_{23}q_{34} + C_1C_4q_{23}q_{34}$; $a_1 = C_4q_{01}q_{12}q_{23} + C_3q_{01}q_{12}q_{34} + C_4q_{01}q_{12}q_{34} + C_2q_{01}q_{23}q_{34} + C_3q_{01}q_{23}q_{34} + C_4q_{01}q_{23}q_{34} + C_1q_{12}q_{23}q_{34} + C_2q_{12}q_{23}q_{34} + C_3q_{12}q_{23}q_{34} + C_4q_{12}q_{23}q_{34}$; $a_0 = q_{01}q_{12}q_{23}q_{34}$ 。

通过上述推导过程得到 FP 参考腔温度变化 \tilde{T}_i 与 \tilde{T}_f 之间的传递函数,再利用传递函数的波德(Bode)图可得到 FP 参考腔的温度敏感度曲线。

3 数值计算

3.1 系统热时间常数计算

对于图 1 所示的真空系统,真空室、热屏蔽层均为

圆柱结构,FP 参考腔为正方体。真空室外径为 200 mm,高度为 200 mm,壁厚为 10 mm。3 个热屏蔽层的顶部和圆周厚度均为 5 mm,底部厚度均为 8 mm。相邻真空室、热屏蔽层的距离均为 10 mm。FP 参考腔边长为 50 mm。真空室材料为不锈钢,热屏蔽层材料为铝合金且表面镀金,FP 参考腔材料为零膨胀玻璃(ULE)。具体材料参数^[20,29]如表 1 所示。

表 1 材料热特性参数

Table 1 Thermal parameters of materials

| Material | Density $\rho /$ ($\text{kg}\cdot\text{m}^{-3}$) | Specific heat capacity $c /$ ($\text{J}\cdot\text{kg}^{-1}\cdot\text{K}^{-1}$) | Thermal conductivity $k /$ ($\text{W}\cdot\text{m}^{-1}\cdot\text{K}^{-1}$) | Radiant emissivity ϵ |
|---|---|---|---|-------------------------------|
| Stainless steel | 7820 | 468 | 13.4 | 0.17 |
| Aluminum alloy (with gold plated surface) | 2700 | 900 | 385 | 0.03 |
| ULE | 2200 | 767 | 1.31 | 0.91 |
| Teflon | 2250 | 1400 | 0.25 | 0.85 |

为了验证式(4)所得的传递函数的正确性,以下分别对仅考虑热辐射和同时考虑热辐射与热传导两种情况进行数值计算与有限元仿真分析。

1) 仅考虑热辐射

初始条件为:系统初始温度 $T_0 = 20^\circ\text{C}$ (293.15 K),真空室外表面温度由 T_0 变为 $T_f = 21^\circ\text{C}$

(294.15 K)。分别由式(1)、式(4)以及 ANSYS 软件计算 FP 参考腔的温度变化,计算结果如图 2 所示。

图 2(a)、(b)为微分方程法与传递函数法的结果对比,图 2(c)、(d)为有限元分析法与传递函数法的结果对比。由图 2 可知,式(1)和式(4)计算得到的 FP 参考腔温度曲线完全吻合,且与 ANSYS 软件计算结果

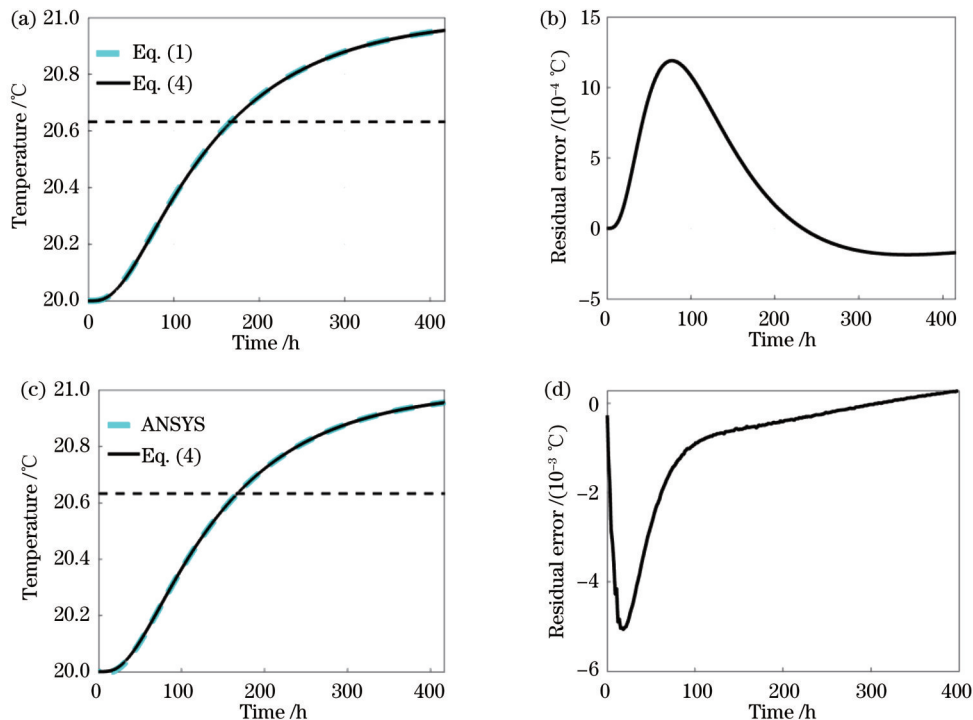


图 2 仅考虑热辐射时 FP 腔温度变化对比。(a)(b)式(1)(微分方程组)与式(4)(传递函数)得出的 FP 腔温度变化对比及残差曲线;
(c)(d) ANSYS(有限元仿真)与式(4)(传递函数)得出的 FP 腔温度变化对比及残差曲线

Fig. 2 Comparison of the temperature change of FP cavity only considering heat radiation. (a)(b) Comparison of temperature change of FP cavity obtained from Eq. (1) (differential equations) and Eq. (4) (transfer function) and its residual error curve; (c)(d) comparison of temperature change of FP cavity obtained from ANSYS (finite element simulation) and Eq. (4) (transfer function) and its residual error curve

十分接近;图 2(b)、(d)所示的残差曲线显示 2 条曲线的差值非常小,可以近似认为 2 条曲线完全重合。当温度到达 $T=(21 - e^{-1})^{\circ}\text{C} \approx 20.632^{\circ}\text{C}$ 时,所对应的时间为系统热时间常数。利用 3 种方法得到的热时间常数分别为 $\tau_1=161.3\text{ h}$ 、 $\tau_2=161.2\text{ h}$ 和 $\tau_3=166.7\text{ h}$ 。式(1)和式(4)计算的热时间常数基本一致,且与 ANSYS 计算结果接近,验证了理论分析、简化推导的

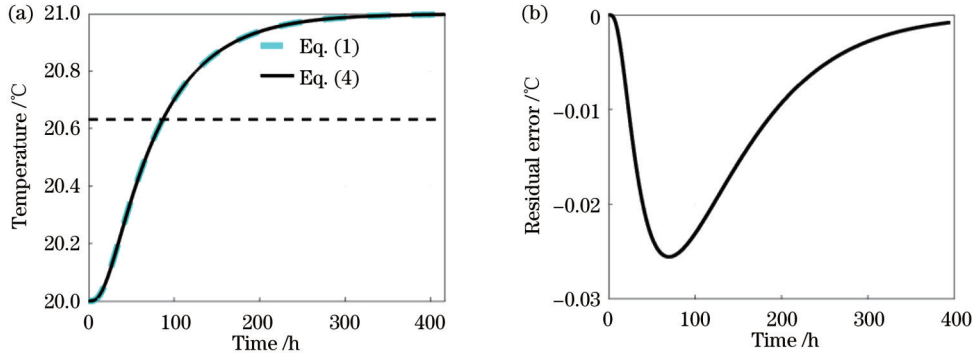


图 3 同时考虑热辐射和热传导时式(1)(微分方程组)与式(4)(传递函数)得出的 FP 腔温度变化曲线对比。(a)FP 腔温度变化对比; (b)残差曲线

Fig. 3 Comparison of temperature change of FP cavity from Eq. (1) (differential equations) and Eq. (4) (transfer function) when simultaneously considering heat radiation and heat conduction. (a) Comparison of the temperature change of FP cavity; (b) residual curve

由图 3 可知,式(1)和式(4)计算得到的 FP 参考腔温度曲线完全重合,残差曲线显示两条温度变化曲线的差值非常小,可以近似认为两条曲线完全重合。利用两种方法得到的热时间常数分别为 $\tau'_1=81.2\text{ h}$ 、 $\tau'_2=81.3\text{ h}$ 。可见:热传导的引入增加了传热途径和传热量,系统热时间常数大幅度降低;由式(1)和式(4)计算的热时间常数基本一致,进一步验证了理论分析、简化推导的正确性。

3.2 参考腔温度敏感度分析

外界温度周期性变化会引起 FP 参考腔温度的周期性变化,其幅值的比值称为 FP 参考腔的温度敏感度。对于一个真空系统而言,FP 参考腔的温度敏感度越低,越有利于保持腔长的稳定性。根据式(4)表示的传递函数绘制 Bode 图,很容易得到 FP 参考腔温度敏感度曲线,其横轴为外界温度抖动的周期,纵轴为温度敏感度。对于热辐射和热传导同时存在的情况,其 FP 参考腔的温度敏感度曲线如图 4 所示。

由图 4 可知,热屏蔽层相当于一个低通滤波器,将外界温度抖动中的高频部分滤除,即外界温度变化越缓慢,对 FP 参考腔温度的影响越明显。当外界温度抖动周期远大于系统热时间常数 ($81.3\text{ h} \approx 2.9 \times 10^5\text{ s}$) 时,FP 参考腔的温度敏感度接近于 1,此时热屏蔽层失去作用。当外界温度在 10^4 s 内变化 1 mK 时,FP 参考腔感受到的温度起伏在 10^{-8} K 量级。

另外,从温度敏感度曲线可知,温度抖动周期小于系统时间常数时,敏感度 y 的对数(以 10 为底)和抖动周期 x 的对数(以 10 为底)之间存在线性关系。这种

正确性。

2)同时考虑热辐射和热传导

在真空室、热屏蔽层以及 FP 参考腔之间增加特氟龙支撑柱,该支撑柱的长度为 10 mm,半径为 5 mm,每层布置 4 个支撑柱,材料参数见表 1。在同样的温度条件下,利用式(1)和式(4)计算 FP 参考腔的温度变化,结果如图 3 所示。

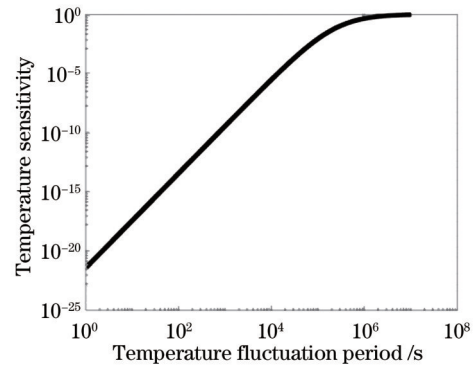


图 4 FP 参考腔温度敏感度曲线

Fig. 4 Temperature sensitivity of FP cavity

关系满足

$$\lg y = b \lg x - d, \quad (5)$$

整理得到

$$y = \frac{x^b}{10^d} = \left(\frac{x}{10^{d/b}} \right)^b. \quad (6)$$

通过对 $x \in [10^0, 10^4]$ 部分曲线的拟合并对系数取整,得到 $b=4$ 、 $d=21$ 。据此,敏感度 y 和抖动周期 x 的关系可表示为

$$y = \frac{x^b}{10^d} = \left(\frac{x}{10^{d/b}} \right)^b = \left(\frac{x}{10^{5.2}} \right)^4. \quad (7)$$

为了建立拟合曲线参数与系统物理参数的关系,通过对比发现,系数 b 与热屏蔽层的层数有关, $10^{d/b} = 10^{5.2}$ 与系统热时间常数 ($2.9 \times 10^5\text{ s}$) 的数值相当,则有

$$y = \left(\frac{x}{\lambda\tau} \right)^{n+1}, \quad (8)$$

式中： τ 为系统热时间常数； n 为系统热屏蔽层数； λ 为修正系数。由于本研究采用了近似手段，因此得出的近似计算公式与理论公式之间存在一定的偏差，而 λ 的引入是为了对本文假设的近似计算公式施加一个修正系数，使得该近似计算公式更加准确合理，并具备被进一步优化的可能性。

由于上述拟合曲线只对 $x \in [10^0, 10^4]$ 部分的曲线进行拟合，综合考虑整个曲线的趋势，可将式(8)写为

$$y = \left(\frac{x}{x + \lambda\tau} \right)^{n+1}. \quad (9)$$

为不失一般性，令 $\lambda = 1$ 。将敏感度的理论计算曲线与式(9)绘制的曲线进行比较，如图5所示。可见，二者虽然存在一定的差异，但式(9)能够简单、快速地估计FP参考腔的灵敏度，在系统设计初期极具参考价值。

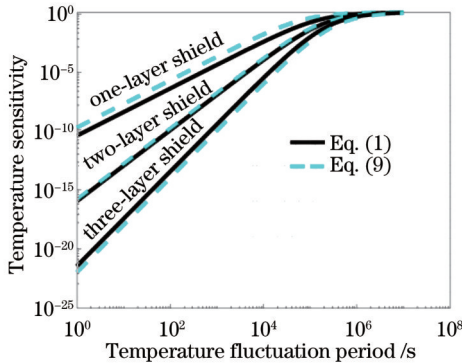


图5 不同屏蔽层数时FP参考腔的温度敏感度曲线

Fig. 5 Temperature sensitivity curves of FP cavity with different multiple layers shield

此外，式(9)仅涉及热屏蔽层数 n 、系统热时间常数 τ 两个参数。由式(9)可知：系统热时间常数越大，热屏蔽层越多，FP参考腔的灵敏度越低；热时间常数相同的系统，其FP参考腔灵敏度不一定相同，而热屏蔽层数多的系统，其FP参考腔的温度敏感度更低。通过调节修正系数 λ 可进一步减小式(9)与理论计算公式的误差， λ 的取值与系统温度、几何参数、材料参数等有关，具体的取值方法还需要进行进一步的研究。

4 结 论

以FP参考腔真空系统为研究对象，针对多个热屏蔽层条件下的FP参考腔温度特性进行理论分析，简化并推导出参考腔温度与外界温度的传递函数关系。仿真对比结果证明了传递函数的正确性，并根据传递函数得到FP参考腔温度敏感度曲线近似计算公式。结果表明，近似公式的计算结果虽然与理论值存在一定差距，但是其形式简单、参数少且直观、计算方便，对

FP参考腔真空系统的初步设计具有很强的指导意义。

参 考 文 献

- [1] Didier A, Millo J, Lacroûte C, et al. Design of an ultra-compact reference ULE cavity[J]. Journal of Physics: Conference Series, 2016, 723: 012029.
- [2] 李铸, 张庆永, 孔令华, 等. 基于激光诱导击穿光谱与随机森林识别GCr15钢的硬度[J]. 中国激光, 2022, 49(9): 0911002. Li Z, Zhang Q Y, Kong L H, et al. Hardness characterization of GCr15 steel based on laser-induced breakdown spectroscopy and random forest[J]. Chinese Journal of Lasers, 2022, 49(9): 0911002.
- [3] Young B C, Cruz F C, Itano W M, et al. Visible lasers with subhertz linewidths[J]. Physical Review Letters, 1999, 82(19): 3799-3802.
- [4] 高军萍, 赵盟盟, 卢嘉, 等. 基于单个强度调制器产生宽光学频率梳系统的研究[J]. 激光与光电子学进展, 2021, 58(9): 0913001. Gao J P, Zhao M M, Lu J, et al. Wide optical frequency comb system based on single intensity modulator[J]. Laser & Optoelectronics Progress, 2021, 58(9): 0913001.
- [5] Prestage J D, Tjoelker R L, Maleki L. Atomic clocks and variations of the fine structure constant[J]. Physical Review Letters, 1995, 74(18): 3511-3514.
- [6] 谈宜东, 徐欣, 张书练. 激光干涉精密测量与应用[J]. 中国激光, 2021, 48(15): 1504001. Tan Y D, Xu X, Zhang S L. Precision measurement and applications of laser interferometry[J]. Chinese Journal of Lasers, 2021, 48(15): 1504001.
- [7] Bloom B J, Nicholson T L, Williams J R, et al. An optical lattice clock with accuracy and stability at the 10^{-18} level[J]. Nature, 2014, 506(7486): 71-75.
- [8] Didier A, Millo J, Marechal B, et al. Ultracompact reference ultralow expansion glass cavity[J]. Applied Optics, 2018, 57(22): 6470-6473.
- [9] Kleppner D. Time too good to be true[J]. Physics Today, 2006, 59(3): 10-11.
- [10] Waldman S J, Collaboration L S. Status of LIGO at the start of the fifth science run[J]. Classical and Quantum Gravity, 2006, 23(19): S653-S660.
- [11] 徐欣, 谈宜东, 穆衡霖, 等. 空间引力波探测中的激光干涉多自由度测量技术[J]. 激光与光电子学进展, 2023, 60(3): 0312006. Xu X, Tan Y D, Mu H L, et al. Laser interferometric multi-degree-of-freedom measurement technology in space gravitational-wave detection[J]. Laser & Optoelectronics Progress, 2023, 60(3): 0312006.
- [12] Wang G F, Li Z, Huang J L, et al. Analysis and suppression of thermal effect of an ultra-stable laser interferometer for space-based gravitational waves detection[J]. Chinese Optics Letters, 2022, 20(1): 011203.
- [13] Fang P C, Sun H Y, Wang Y, et al. Transfer of laser frequency from 729 nm to 1.5 μm with precision at the level of 10^{-20} [J]. Chinese Optics Letters, 2022, 20(8): 081403.
- [14] Wang K, Tian H C, Meng F, et al. Fiber-delay-line-referenced optical frequency combs: three stabilization schemes[J]. Chinese Optics Letters, 2022, 20(2): 021204.
- [15] Webster S, Gill P. Force-insensitive optical cavity[J]. Optics Letters, 2011, 36(18): 3572-3574.
- [16] Black E D. An introduction to Pound-Drever-Hall laser frequency stabilization[J]. American Journal of Physics, 2001, 69(1): 79-87.
- [17] Chen L S, Hall J L, Ye J, et al. Vibration-induced elastic deformation of Fabry-Perot cavities[J]. Physical Review A, 2006, 74(5): 053801.
- [18] Millo J, Magalhães D V, Mandache C, et al. Ultrastable lasers

- based on vibration insensitive cavities[J]. *Physical Review A*, 2009, 79(5): 053829.
- [19] Xu G J, Jiao D D, Chen L, et al. Analysis of vibration sensitivity induced by the elastic deformation of vertical optical reference cavities[J]. *IEEE Access*, 2020, 8: 194466-194476.
- [20] Dai X J, Jiang Y Y, Hang C, et al. Thermal analysis of optical reference cavities for low sensitivity to environmental temperature fluctuations[J]. *Optics Express*, 2015, 23(4): 5134-5146.
- [21] Zhang J, Wu W, Shi X H, et al. Design verification of large time constant thermal shields for optical reference cavities[J]. *The Review of Scientific Instruments*, 2016, 87(2): 023104.
- [22] Dubé P, Madej A A, Bernard J E, et al. A narrow linewidth and frequency-stable probe laser source for the $^{88}\text{Sr}^+$ single ion optical frequency standard[J]. *Applied Physics B*, 2009, 95(1): 43-54.
- [23] Sanjuan J, Gürlebeck N, Braxmaier C. Mathematical model of thermal shields for long-term stability optical resonators[J]. *Optics Express*, 2015, 23(14): 17892-17908.
- [24] 伍巍. 超稳激光真空系统热时间常数的研究[D]. 武汉: 华中科技大学, 2016.
- Wu W. Research on thermal time constants of vacuum chamber systems for ultra-stable lasers[D]. Wuhan: Huazhong University of Science and Technology, 2016.
- [25] 杨世铭, 陶文铨. 传热学[M]. 4 版. 北京: 高等教育出版社, 2006.
- Yang S M, Tao W Q. Heat transfer[M]. 4th ed. Beijing: Higher Education Press, 2006.
- [26] 姚仲鹏, 王瑞君. 传热学[M]. 2 版. 北京: 北京理工大学出版社, 2003.
- Yao Z P, Wang R J. Heat transmission science[M]. 2nd ed. Beijing: Beijing Institute of Technology Press, 2003.
- [27] Green D W, Southard M Z. Perry's chemical engineers' handbook[M]. 9th ed. New York: McGraw-Hill Education, 2019.
- [28] Ahmed W. Advantages and disadvantages of using MATLAB/ode45 for solving differential equations in engineering applications[J]. *Computer Science Journals*, 2013, 7(1): 27.
- [29] 李雪艳, 蒋燕义, 姚远, 等. 环境温度变化不敏感的光学腔热屏蔽层设计[J]. *光学学报*, 2018, 38(7): 0714002.
- Li X Y, Jiang Y Y, Yao Y, et al. Design of thermal shield of optical cavities for low sensitivity to environmental temperature fluctuations[J]. *Acta Optica Sinica*, 2018, 38(7): 0714002.

Thermal Analysis Method for Optical Reference Cavity of Ultra-Stable Laser Based on Transfer Function

Deng Jiuchang^{1,2}, Xie Yong¹, Meng Lingqiang^{2,3**}, Bian Wei², Yin Xiongfei², Jia Jianjun^{1,2,3*}

¹Key Laboratory of Space Active Optical-Electro Technology, Shanghai Institute of Technical Physics, Chinese Academy of Sciences, Shanghai 200083, China;

²Taiji Laboratory for Gravitational Wave Universe, Key Laboratory of Gravitational Wave Precision Measurement of Zhejiang Province, School of Physics and Photoelectric Engineering, Hangzhou Institute for Advanced Study, University of Chinese Academy of Sciences, Hangzhou 310024, Zhejiang, China;

³Research Center for Intelligent Sensing Systems, Zhejiang Laboratory, Hangzhou 311121, Zhejiang, China

Abstract

Objective Ultra-stable laser has excellent characteristics such as extremely low frequency noises and extremely high coherence, and it is widely used in cold atomic light clocks, geodesy, gravitational wave detection, and optical frequency transmission. When the laser frequency is locked on the Fabry-Pérot (FP) cavity using Pound-Driver-Hall (PDH) frequency stabilization technology, the frequency stability of the laser depends entirely on the cavity length stability of the cavity. The temperature fluctuation of the FP cavity is one of the main factors that affect the cavity length. How to quickly analyze its temperature characteristics has been the research focus of ultra-stable lasers. The cavity length change of the FP cavity is mainly affected by the temperature fluctuation of the external environment. To suppress this effect, researchers both in China and abroad usually place the cavity in a vacuum chamber with multi-layer thermal shields to obtain a larger thermal time constant and a lower temperature sensitivity. Therefore, to quickly and accurately analyze the influence of the thermal shield parameters in the vacuum chamber on the temperature of the FP cavity, global researchers have carried out corresponding research based on various thermal analysis methods, such as the transfer function method, finite element analysis method, and direct differential method. At present, most of the thermal analysis methods of the FP cavity system only focus on the law of the temperature of the cavity changing with time, and the research results of the temperature sensitivity of the FP cavity required by the actual working conditions cannot meet the urgent needs of the actual working conditions. Therefore, this paper proposes a thermal analysis method of the FP cavity after comprehensively considering heat conduction and radiation and establishes the relationship between temperature sensitivity and corresponding physical parameters of the system, which can guide the design of the FP cavity system in practical engineering.

Methods In this paper, a typical FP cavity vacuum system is taken as the research object. Through theoretical analysis,

the differential equations between the FP cavity's temperature and the external temperature under heat conduction and radiation are derived. According to the differential equations, the transfer function relationship between the FP cavity's temperature and the external temperature is derived by using a reasonable simplified approximation method. The correctness of the transfer function relationship is proved by numerical calculation and finite element simulation. On the basis of the temperature sensitivity curve obtained from the Bode plot of the transfer function, a simplified approximate formula for calculating the temperature sensitivity of the FP cavity is proposed. By combining the overall trend of the curve and considering the wide applicability of the approximate formula, the proposed approximate formula is improved and revised. Finally, the curve obtained from the approximate formula is compared with that obtained from the theoretical formula by numerical calculation. The results show that the overall trend of the curves obtained by the two methods is completely consistent, although there are some small errors.

Results and Discussions In this paper, the transfer function relationship between the FP cavity's temperature and the external temperature is derived by reasonably simplifying the approximation method. Through the analysis and comparison of numerical calculation and finite element analysis methods, it can be concluded that the temperature curve of the FP cavity obtained by this transfer function is completely consistent with the one obtained by the theoretical formula, and it is very close to the calculation result of ANSYS software under both the condition of only considering heat radiation [Figs. 2(a) and 2(c)] or considering heat conduction and radiation comprehensively [Fig. 3(a)]. The residual curves [Figs. 2(b), 2(d), and 3(b)] given in the paper show that the difference between the curves is very small, and it can be approximately considered that the curves are completely consistent. The calculation results of the two formulas for the thermal time constant are consistent and very close to those of the ANSYS software. Based on the temperature sensitivity curve of the FP cavity (Fig. 4), this paper gives a simplified approximate formula for calculating the temperature sensitivity of the cavity. The comparison between the curve obtained from the approximate formula and that obtained from the theoretical formula shows (Fig. 5) that the overall trend of the curves is completely consistent. Although there are some errors, the sensitivity approximate formula has the characteristics of simple form, intuitional parameters, and convenient calculation, and it is of important guiding significance for the design of the ultra-stable laser system.

Conclusions In this paper, the FP cavity vacuum system is taken as the research object, and the temperature characteristics of the FP cavity under multi-layer thermal shields are analyzed theoretically. The transfer function relationship between the FP cavity's temperature and the external temperature is simplified and deduced. The simulation results show that the transfer function formula is correct. According to the transfer function, the approximate formula for fitting the temperature sensitivity curve of the FP cavity is obtained. The results show that although there are some differences between the approximate formula and the theoretical value, the approximate formula has the characteristics of simple form, intuitional parameters, and convenient calculation, and it is of strong guiding significance for the preliminary design of the FP cavity vacuum system.

Key words laser optics; FP cavity; transfer function; thermal shield; temperature sensitivity